

Seismotectonic activity in East Belgium: relevance of a major scarp and two associated landslides in the region of Malmedy

Anne-Sophie MREYEN^{1*}, Alain DEMOULIN² & Hans-Balder HAVENITH¹

¹ University of Liege, Department of Geology, Allée du six Août 14, B18, 4000 Liege, Belgium.

² University of Liege, Department of Physical Geography, Clos Mercator 3, B11, 4000 Liege, Belgium.

*corresponding author: AS.Mreyen@uliege.be.

ABSTRACT. Geomorphological markers such as scarps, river diversions and slope failures can be used as proxy indicators for the seismotectonic activity of a region. This study concentrates on the Malmedy-Bévercé area, E-Belgium, where formerly unknown geomorphological features have been recently discovered in the frame of a new regional geological mapping campaign. The area is characterised by gentle to locally very steep slopes along the Warche valley crossing the Stavelot Massif and the Malmedy Graben. Coupled with a LiDAR-DEM and UAV imagery analysis, field mapping has revealed a steep scarp extending near two landslides on the southern hillslopes of the Warche valley at Bévercé. These slope failures developed in the Permian conglomerates of the Malmedy Formation (also known as the *Poudingue de Malmedy*), which represent the infill of the Malmedy Graben. Roughly perpendicular to the graben axis, the scarp has a N330°E orientation similar to that of the seismotectonically active Hockai Fault Zone that crosses the Malmedy region in this area. In this paper, we present the geological and geomorphological context of the Bévercé scarp and of the largest landslide. Furthermore, we demonstrate the results of a geophysical reconnaissance survey of the structures (seismic refraction and electrical resistivity profiling). The geophysical results highlight a vertical displacement of the seismic layers and laterally changing electrical properties across the scarp, with very low resistivity values in its middle part. A low resistivity zone in the subsurface can also be found within the larger landslide, right in the prolongation of the scarp. All these observations hint at the presence of a major, probably seismically active, fault belonging to the eastern border of the Hockai Fault Zone.

KEYWORDS: Hockai Fault Zone, tectonic scarp, geomorphological analysis, LiDAR-DEM, seismic and electrical tomography, ancient mass movements.

RÉSUMÉ. L'activité sismotectonique dans l'Est de la Belgique : l'intérêt d'un escarpement majeur et de deux glissements de terrain dans la région de Malmedy. Les marqueurs géomorphologiques, tels que les escarpements, les détournements de rivières et les ruptures de pente, peuvent être utilisés comme indicateurs indirects de l'activité néotectonique d'une région. Cette étude se concentre sur la région de Malmedy-Bévercé, dans l'Est de la Belgique, où des structures géomorphologiques, autrefois inconnues, ont été découvertes récemment, dans le cadre de la dernière campagne de cartographie géologique. La région se caractérise par des pentes douces à localement très raides le long de la vallée de la Warche, traversant le massif de Stavelot et le graben de Malmedy. Couplé à une analyse d'imagerie LiDAR-DEM et drone, la cartographie de terrain a révélé un escarpement abrupt s'étendant près de deux ruptures de pente sur les versants sud de la vallée de la Warche, à proximité du village de Bévercé. Les instabilités de pente se sont développées dans le conglomérat permien, connu sous le nom du Poudingue de Malmedy (ou Formation de Malmedy), qui représente le remplissage sédimentaire fluvial du Graben de Malmedy. Avec une direction N330°E, l'escarpement en question est quasiment perpendiculaire aux structures connues dans le graben, mais parallèle à l'orientation de la Zone de Faille de Hockai sismiquement active qui traverse la région de Malmedy à cet endroit. Dans cet article, nous présentons d'abord le contexte géologique et géomorphologique de l'escarpement et des glissements de terrain. Ensuite, nous montrons les résultats d'une campagne géophysique (comportant deux profils sismiques et deux profils électriques) qui a été réalisée sur ces structures. Les profils géophysiques obtenus montrent un déplacement vertical des couches sismiques ainsi que des changements latéraux des résistivités à travers de l'escarpement. Une zone de faible résistivité a pu être observée à l'intérieur de cet escarpement, ainsi que dans le plus grand des deux glissements de terrain, exactement dans le prolongement de l'escarpement. Toutes ces observations sont indicatrices de la présence d'une faille importante, probablement sismiquement active, faisant partie du bord est de la Zone de Faille de Hockai.

MOTS-CLÉS : Zone de Faille de Hockai, escarpement tectonique, analyse géomorphologique, MNT LiDAR, tomographie sismique et électrique, anciens mouvements de masse.

ZUSAMMENFASSUNG. Seismotektonische Aktivität in Ostbelgien: Relevanz eines Steilhangs und nebenliegender Hangrutschungen in der Region Malmedy. Geomorphologische Merkmale wie Steilhänge, Flussumleitungen und Hangrutschungen können als Proxy-Indikatoren der seismotektonischen Aktivität einer Region genutzt werden. In dieser Arbeit konzentrieren wir uns auf die Malmedy-Bévercé Region, Ostbelgien, in der kürzlich, zuvor unbekannte, geomorphologische Strukturen während geologischer Kartierungsarbeiten entdeckt wurden. Die Region ist von seichten bis lokal recht steilen Hängen entlang des Warche-Tals innerhalb des Malmedy Grabens und des Stavelot Massifs gekennzeichnet. Die geologische Feldkartierung konnte dort, zusammen mit Analysen eines LiDAR-DGMs und Drohnenaufnahmen, einen markanten Steilhang, sowie zwei Hangrutschungen an den südlichen Hängen des Warche-Tals in der Nähe der Ortschaft Bévercé aufdecken. Die dabei betroffene Gesteinsformation ist ein permisches Konglomerat, auch *Poudingue de Malmedy* genannt, welches die sedimentäre Füllung des Malmedy Grabens darstellt. Der charakteristische Steilhang ist mit einer Orientierung von N330°E annähernd senkrecht zu den Hauptstrukturen des tektonischen Grabens ausgerichtet und folgt somit der Orientierung der seismotektonisch aktiven Hockai-Störungszone, die die Region Malmedy durchquert. In diesem Artikel präsentieren wir zunächst den geologisch-geomorphologischen Kontext des Bévercé Steilhangs und der größeren Hangrutschung. Anschließend werden die Resultate einer kleinen geophysikalischen Studie (seismische Refraktions- und elektrische Resistivitätstomographien) entlang des Steilhangs und der nebenliegenden Rutschung beschrieben. Diese zeigen einen vertikalen Versatz der seismischen Einheiten, sowie eine laterale Veränderung der elektrischen Widerstände mit besonders niedrigen Werten innerhalb des Steilhangs auf. Eine solche Zone niedriger Widerstände wurde auch im größeren Bévercé-Rutsch gefunden, und zwar in der direkten Verlängerung des Steilhangs. All diese Beobachtungen weisen auf die Präsenz einer größeren, wahrscheinlich seismisch aktiven, Verwerfung hin, die somit zum östlichen Rand der Hockai-Störungszone gehört.

SCHLÜSSELWÖRTER: Hockai-Störungszone, Störungsausschnitt, geomorphologische Analyse, LiDAR-DGM, seismische und elektrische Tomographie, alte Massenbewegungen.

1. Introduction

For the characterisation of a region's seismotectonic activity, it is important to study its distinct geomorphological markers, e.g. tectonic scarps, alignments, river diversions, etc., that can serve as proxy indicators for past tectonic movements. Also slope failures and landslides can be used as relevant proxies for seismotectonics, especially in regions known to be seismically active. To clearly identify these markers in their regional context, we strongly depend on field accessibility for geological-geomorphological and geophysical analyses, but also on high resolution topographic data. For the latter, airborne LiDAR (Light Detection and Ranging) technology offers new insights into a highly detailed scale, and is especially advantageous in forested areas (e.g. Challis et al., 2011; Lin et al., 2013; Cunningham et al., 2006).

In the region of Malmédy, East Belgium, a steep scarp together with slope failure morphologies were discovered and highlighted by the geologists responsible for the revision of the Stavelot – Malmédy geological map (Lamberty et al., in press) as part of the Mapping Revision Program for the Geological Survey of Wallonia, commissioned by the Public Service of Wallonia (SPW-DGO3) at the Universities. A series of studies have been carried out before in order to analyse the geomorphology and neotectonics of this region (see, e.g., Demoulin, 2006 and Lecocq, 2011), but the scarp and the two landslides were 'unknown' before 2015. This work aims at describing the scarp and the bigger of both landslides in detail, and at establishing their origin in the tectonic context of the region. To carry out this objective, we focus on the combination of different methods, i.e. analyses on the basis of a high resolution LiDAR-DEM and UAV imagery together with the geophysical reconnaissance of the scarp and the directly adjacent landslide.

In the following, we present a detailed geomorphology survey of the failed slopes, together with the results of a small

geophysical survey that was completed on the scarp and adjacent landslide. By combining our results with formerly acquired regional data and interpretations (Demoulin, 2006; Lecocq, 2011), we will then provide some interpretations of the origin of the scarp and the causes of landsliding.

2. Study area

The two older landslides found in East Belgium (see location in Fig. 1a), near the eastern end of the Malmédy Graben, developed on relatively pronounced slopes in the southern part of the Warche valley in Bévécé. The larger of both, here called Bévécé landslide, lies directly next to a NNW-striking steep scarp with a height of ~20 m and a length of ~100 m. The analysis of the new LiDAR-DEM of the area (SPW, 2015) unequivocally confirmed the presence of these two landslides and the nearby scarp (Fig. 1b). Heavy storms in 2014 devastated the dense forest cover of the landslides and the subsequent clearing of the slopes exposed the landslide morphology and facilitated their access. Figures 1c-d show orthophotos with the forest cover of the region in the past, while the orthophoto in Figure 1e was taken in 2015 when deforestation had already started.

Earlier regional works (Renier, 1902; Antun, 1954; Ozer & Macar, 1968; Ozer, 1979; Prick & Ozer, 1995) neither identified the scarp nor the two large landslides. However, Ozer (1967) mapped a small shallow landslide (a few tens of square meters, 2-3 m thick) in the same area, which he tentatively interpreted as an earth flow caused by infiltration of precipitation water.

2.1. Tectonic context of the region

The wider tectonic context of the study area is defined by the Stavelot Massif hosting the Malmédy Graben (introduced by Geukens, 1957). As a consequence of late Variscan deformation affecting the region, the ENE-WSW striking graben structure

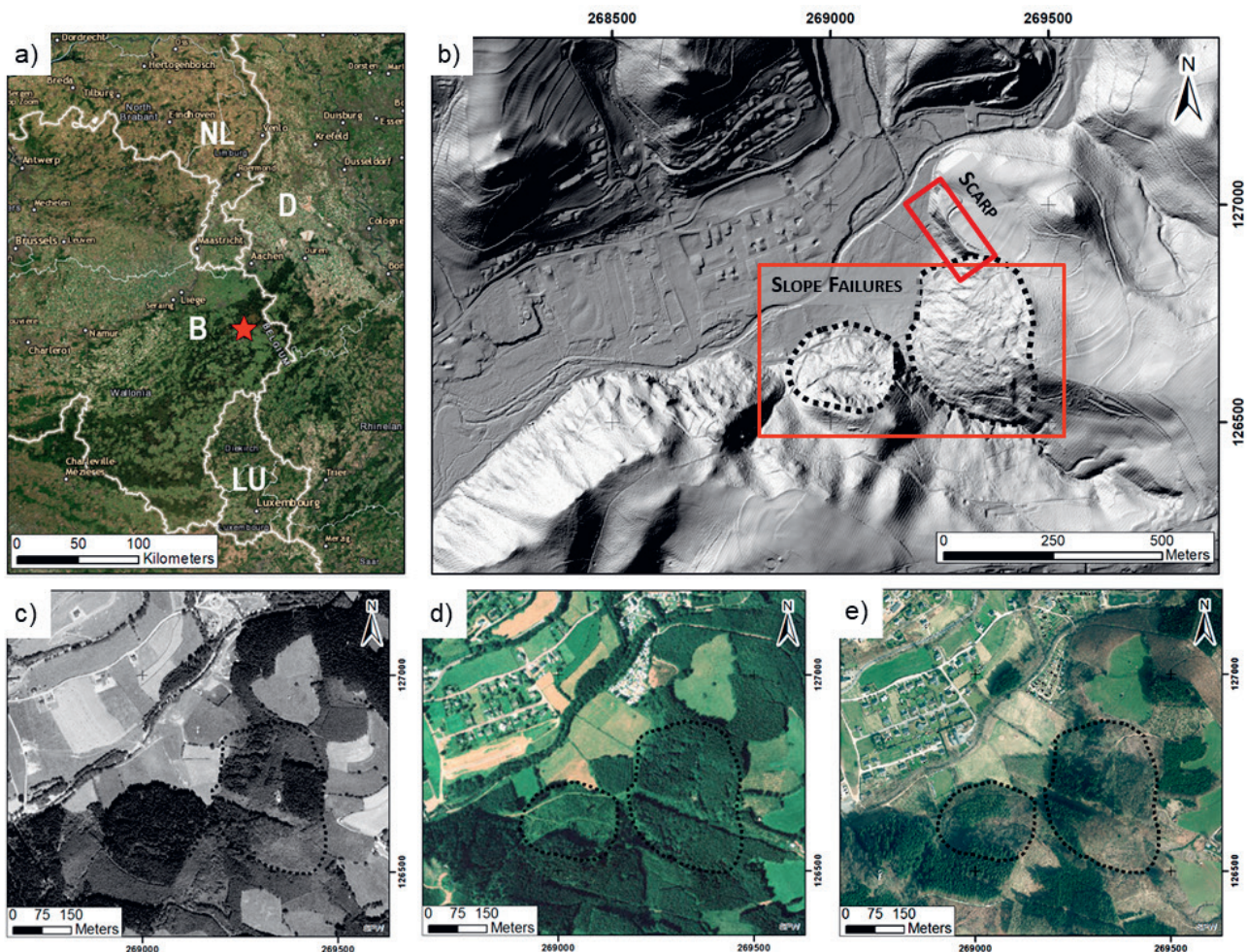


Figure 1. a) Location of the study area in East Belgium. b) Hillshade on the basis of LiDAR-DEM revealing the scarp and the landslides in the Malmédy-Bévécé region. Orthophotos showing the evolution of forest cover in the study area from the years 1971 (c), 1994-2000 (d), and 2015 (e) after several heavy storms and deforestation (SPW, 2015).

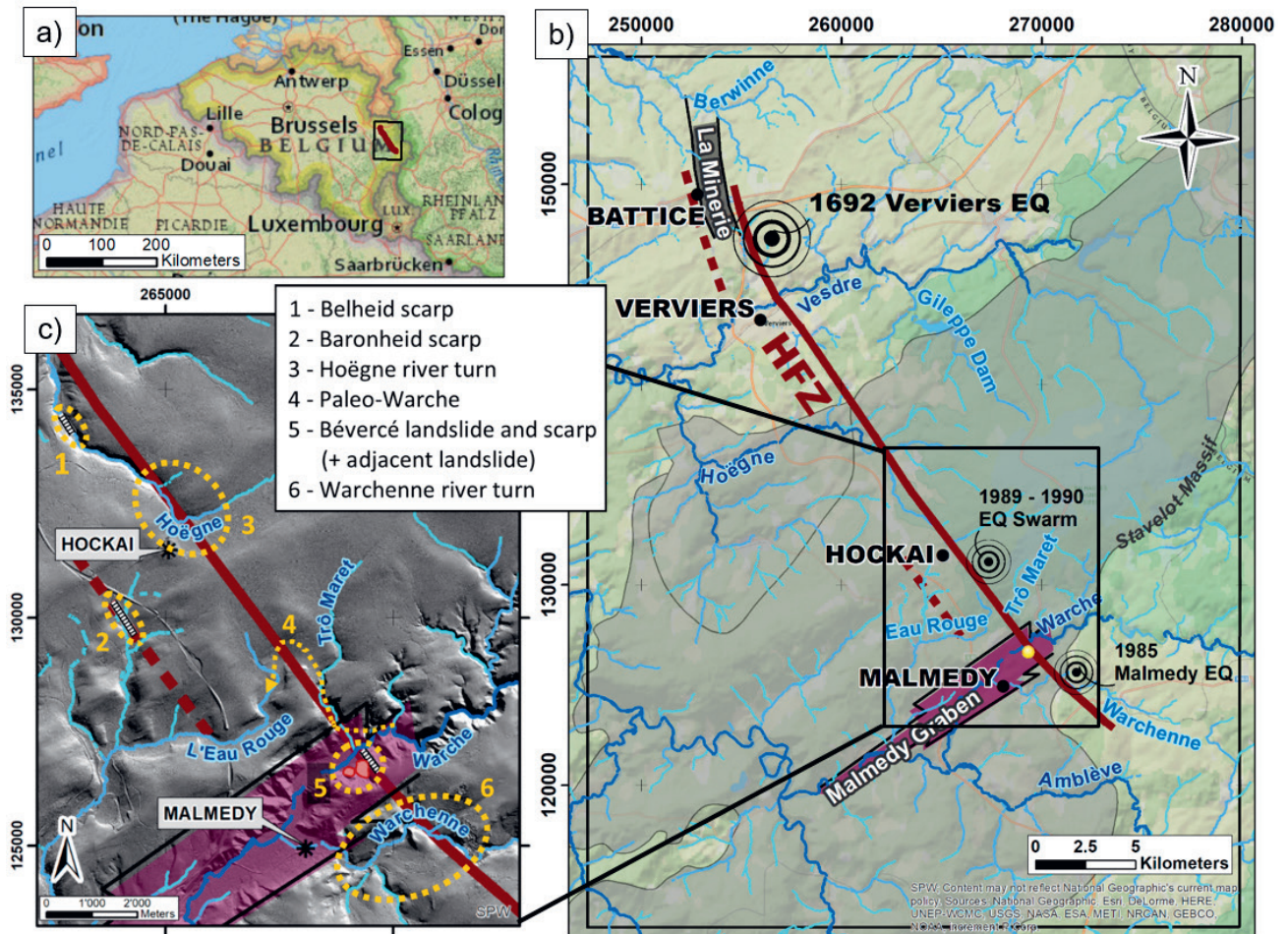


Figure 2. a) Situation of the Hockai Fault Zone (HFZ) in East Belgium. b) Outline of the HFZ after Demoulin (2006) crossing the Stavelot Massif and the Malmedy Graben (with the study area marked by a yellow dot in the Malmedy Graben). The hatched lines parallel to the HFZ refer to parallel supposed tectonic markers (i.e. western part of the conjugate faults within the Minerie Graben in the North and the E-oriented Baronheid scarp in the South; Lecocq, 2011). c) Detailed geomorphological expressions in the SE part of the HFZ (scarps, landslides and river diversions). HFZ geomorphic markers ‘1’ to ‘6’ are outlined and shortly described in the text.

formed in the middle part of the Stavelot Massif. The 25 km long and approximately 2.5 km wide depression is filled with a Permian reddish conglomerate, called the Malmedy Formation or *Poudingue de Malmedy* (see location and geological overview maps in Fig. 2). The Bévercé scarp and landslides developed in this conglomerate formation that lies discordant on top of Cambro-Ordovician bedrock.

Furthermore, the tectonics of the region are marked by the presence of the 42 km long and seismically active Hockai Fault Zone (HFZ; Ahorner, 1983; Demoulin, 1988). In contrast to the prevailing Variscan direction (i.e. N50-60°E), the HFZ is dominated by a N330°E orientation. The ruptured zone significantly marks the geomorphology of the region; Demoulin (2006) and Lecocq (2011) describe its numerous morphological expressions that can be found between the regions of Battice and Malmedy-Waimes, East Belgium (Figs 2a and 2b).

In terms of seismicity, the HFZ most likely produced the historical September 18, 1692, Verviers earthquake (Ms 6 – 6.3; Camelbeeck et al., 2000; Alexandre et al., 2008) in its northern part. The 1692 earthquake predominantly affected the northern Belgian Ardennes, but is also known as the strongest historical seismic event in north-western Europe with effects perceivable from Kent in England, to the Rhineland in Germany as well as to the Champagne in France. Since the beginning of the digital instrumental recording of seismic activity, 103 smaller earthquakes with hypocentral depths ranging from 5 to 10 km could be located inside the HFZ: in 1985, a M_L 2.9 event occurred in the region of Malmedy; a few years later, between 1989 and 1990, a seismic sequence (with events of $M_L = 1.0 - 2.4$) was recorded along a 12 km long zone in the North-East of Malmedy (see epicenter locations in Fig. 2b; Camelbeeck, 1993; Lecocq, 2011; Vanneste et al., 2018).

The HFZ comprises faults of strike-slip and normal displacement components; it furthermore presents multiple geological and geomorphological markers such as scarps, bedrock displacements and river diversions. The northern part of the zone, more precisely the *Pays de Herve* in the region of Battice, is marked by the Minerie Graben (*La Minerie* in Fig. 2b; Forir, 1905; Ancion & Evrard, 1957), but also by the presence of landslides (Barchy & Marion, 2000; Demoulin et al., 2000, 2003; Demoulin & Glade, 2004; Demoulin & Chung, 2007; Dewitte et al., 2018). Figure 2c highlights the geomorphological impact of the HFZ in the SE part with the presence of (assumed) surface ruptures such as the *Belheid* (marked ‘1’ in Fig. 2c) and *Baronheid* scarps (‘2’; Lecocq, 2011). Furthermore, the tectonic impact of the fault system affected local river systems by watercourse diversions and flow direction changes in this region: The Hoëgne (‘3’) as well as the Warchenne (‘6’) rivers changed their watercourse by nearly 90° along the orientation of the HFZ border faults.

An important river capture occurred in the direct vicinity of our study area, the one of the Warche River. The current watercourse of the Warche River in the Malmedy region is joined by the Trô Maret River and subsequently passes through Bévercé and Malmedy from East to West. Before finally running into the Amblève River, it flows together with the Warchenne in the South of Malmedy. Prior to river capturing, the Warche was flowing along the valleys that are nowadays occupied by the Trô Maret, Les Chôdières and L’Eau Rouge (also known as “Paleo-Warche”; Pissart & Juvigné, 1982; Delvenne et al., 2004; Juvigné & Delvenne, 2005; Rixhon & Demoulin, 2018). Demoulin et al. (2004) consider the tectonic influence of the HFZ as responsible for the previous detour through the quite competent upper Cambrian rocks (Revin group). The present course of the Warche is thereby most probably due to a capture of the river by a smaller one that was retrogressively

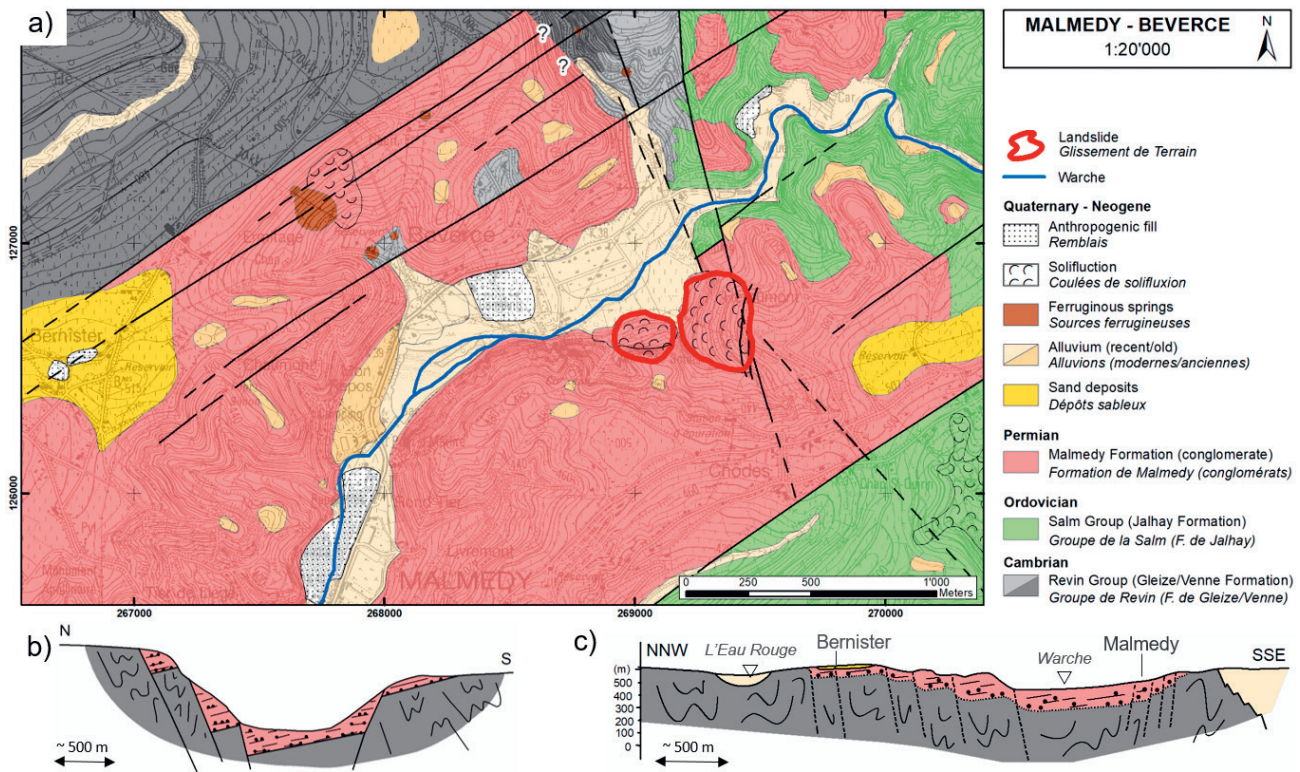


Figure 3. a) Extract of the Stavelot – Malmedy geological map of the Malmedy-Bévercé region (modified from Lamberty et al., in press; Belgian Lambert 72 projection), note question marks refer to uncertain lithological limits of the Malmedy Formation. b) Schematic N-S profile across the Malmedy Graben (modified from Geukens, 1995 – no precise location known, but likely to be close to the target area as it indicates a small thickness in the lower parts of the graben). c) Cross section of the Malmedy Graben through the areas of Bernister and Malmedy (modified from Lamberty et al., in press) that are located directly in the West of the map shown in (a).

eroding the conglomerate filling of the Malmedy Graben, from West to East, before finally reaching the turn of the Warche (about 50,000 – 80,000 years ago; Juvigné & Schumacker, 1985; Juvigné & Delvenne, 2005; Vanneste et al., 2018) not far from the present-day confluence of the Warche River and the Trô Maret River – and so very close to the scarp site.

2.2. Geological context of the study area

The local geology of the study area is characterised by the sediment filling of the Malmedy Graben, notably the rock formation in which the landslides developed. The scarp affects this formation as well, but its basis is partly located within the bedrock. The Malmedy Formation is a Permian conglomerate composed of alluvial pebbles in a reddish matrix (Dumont, 1832; Renier, 1902; Antun, 1954). It can be described as a hard rock formation due to its predominantly calcareous characteristics (especially in the so called “Middle Member”, predominantly present in the Malmedy-Bévercé region; Renier, 1902). The layering generally dips by 10° (to 15°) towards NNW (Geukens, 1957, 1995; Bless et al., 1990; Lamberty et al., in press), whereby the origin of the stratification is related to the natural deposition of the clasts within the matrix. These allochthonous clasts can be described as mostly well rounded pebbles of varying composition and diameter (up to 60 cm). The argillaceous to argillaceous-calcareous cementation can be affected by fracture networks inducing high permeability as well as good drainage capacities throughout the rock. Also, the formation can contain intercalated layers of fine grained sediments, such as sandy to silty-argillaceous beds. The subjacent quartzite and phyllite bedrock of the region is of Cambro-Ordovician age and belongs to the Deville, Revin and Salm groups (Renier, 1902; Bless et al., 1990; Lamberty et al., in press). According to Ozer (1967), the high permeability of the *Poudingue* leads to internal erosion processes that can cause weathering phenomena along the bedrock contact.

Figure 3a presents an extract from the newly established geological map of the study area (Lamberty et al., in press) showing the recently detected slope failures in their geological setting. Figures 3b and 3c show two geological cross sections of

the Malmedy Graben from different authors, which provide an overview on its internal structure and lithological contacts.

3. Methodology

3.1. Geomorphological analysis of the study area

In order to better understand the study area, a geomorphological analysis was performed in the field as well as based on imagery data (by means of a high resolution LiDAR data and UAV photography). Here, we focus on the larger of the two aforementioned landslides, the ‘Bévercé landslide’. Several outcrops of the conglomerate formation (and also bedrock in the scarp area) were investigated in terms of layer strike and dip in order to retrace possible translational or rotational movements of blocks and subareas. Field observations were mapped, digitised and later compared to the 1 m resolution LiDAR-DEM of the study area. The latter was created on the basis of LiDAR (Light Detection and Ranging) data collected by the Public Service of the Walloon Region (SPW) during the years 2012–2014. It was further used to analyse the region in terms of curvature and slope characteristics with GIS software.

3.2. Geophysical prospection of the scarp and adjacent landslide

In combination with the geomorphological analyses, a geophysical study was carried out on the site in order to examine the nature of the Bévercé scarp. For this, two profile lines crossing the scarp and one crossing the landslide body were selected for geophysical measurements. For the scarp area, seismic refraction and electrical resistivity measurements were completed and processed as 115 m long tomographic profiles (SRT – Seismic Refraction Tomography and ERT – Electrical Resistivity Tomography). The methods were validated by comparing both survey results along the same two profile locations. For the detection of a possible weak zone within the adjacent landslide area, we completed an additional longer ERT profile.

For the SRT profiling (SP05 and SP06), seismic wave recording was performed with 24 4.5 Hz geophones (5 m spacing, 115 m profile length) connected to a 16-bit 24 channel

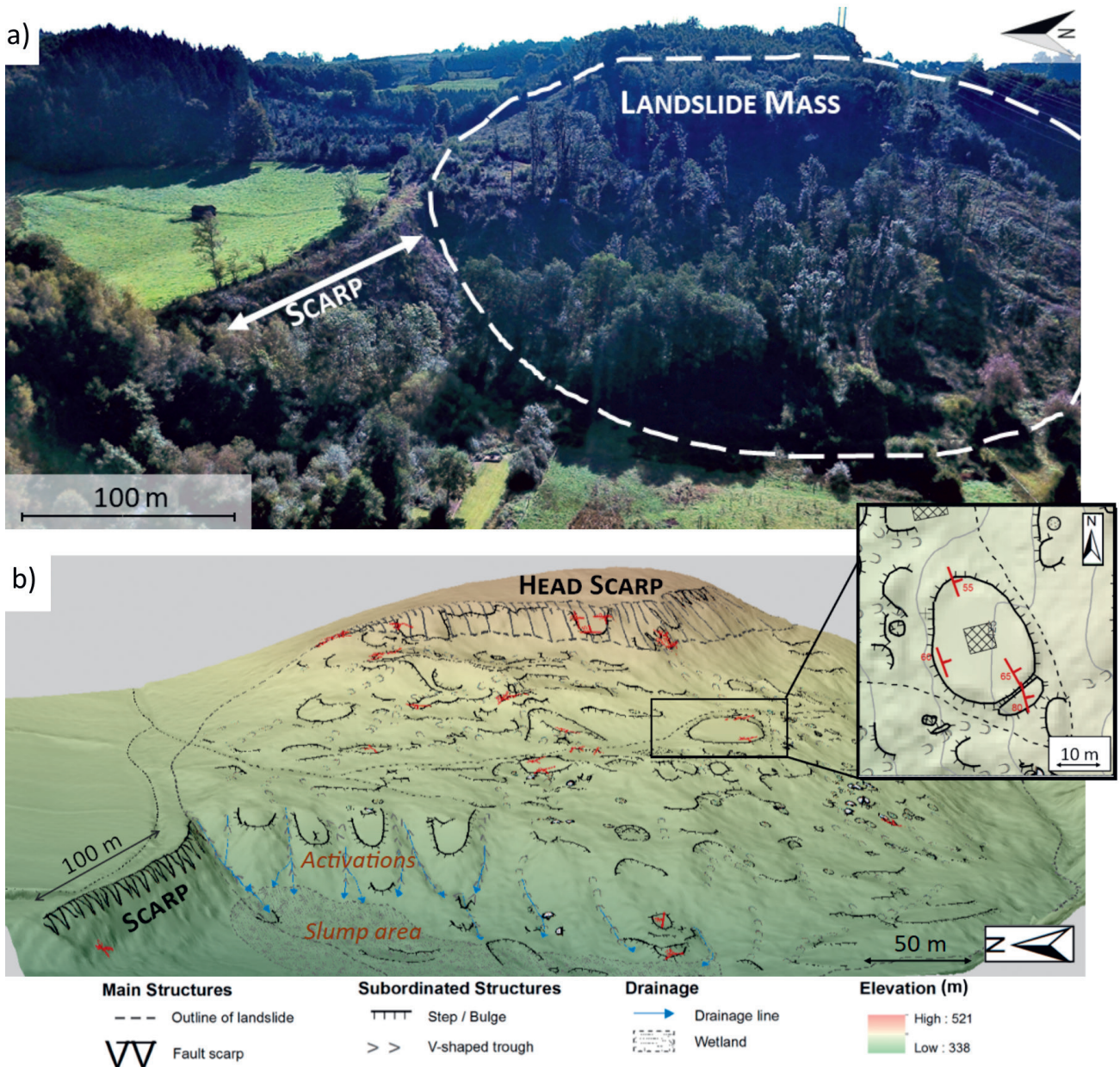


Figure 4. a) UAV photo of the study area with scarp and landslide. b) Geomorphological map of the Bévercé landslide projected on a 3D geomodel (created with the GOCAD Software by Paradigm, on the basis of the LiDAR-DEM) with detailed view of an important block tilted backward (bedding towards E instead of normal dip toward the W; local dip of layer presented by the red strike and dip symbols).

seismograph (DAQLinkII). The required seismic energy was triggered by sledgehammer impacts on a metal plate at various shot points along the profiles. Each of the seismic surveys was analysed in terms of P-wave travel times with the SARDINE software developed by Demanet (2000).

For the ERT profiles ERT03 and ERT04, a total of 24 electrodes connected to an IRIS Instruments Syscal Switch-24 resistivity meter were set up (5 m spacing, 115 m profile length). For the ERT02 profile across the landslide, an ABEM system connected to 4 cables with 16 electrodes each, and a 5 m spacing between electrodes, was used (total profile length of 315 m). The apparent resistivity data of the subsoil were processed as 2D electrical resistivity tomography by using the 2D inversion algorithm of Loke & Barker (1996) implemented in the RES2DINV software (Geotomo Software). We here present results processed in the Wenner electrode configuration (i.e. with equal distances between A-M, M-N, and N-B electrodes; Loke, 2004).

4. Results

The landslide is assumed to be relatively deep-seated with an approximate surface area of 80,000 m² and an estimated volume of 600,000 to 1,000,000 m³. Geomorphological observations

suggest that it is relatively old (>>100 years), as its hummocky surface structures are relatively smooth and as relatively large trees were found within the failed zone. Moreover, a small house built in the central part during the sixties has not been affected by any deformations.

Together with UAV imagery taken by our team, typical landslide surface morphologies observed in the field can be underlined, such as the pronounced head scarp and parallel counter slope along the graben, as well as hummocky structures along the slope. Figure 4a shows a recent UAV photo of the scarp (view towards ESE) next to the landslide surface. Within the landslide area, geomorphological and geological observations reveal diverse structures evidencing a pronounced slope failure. The geomorphological observations are summarised in the form of a geomorphological map of the area (Fig. 4b). The landslide area can be subdivided, from top to bottom, into a head scarp with zone of depletion, the main area of deposit with a hummocky surface, a swamp area at the foot of the slope and a zone of internal activations in the NW part of the slope. The latter could also be the consequence of forest clearing, inducing local activations along the slope.

Figure 5a presents the location of geophysical profiles and points of structural observations shown in Figure 5b. Along

the scarp, the outcropping of Permian conglomerate is in direct vicinity (at the same altitude) of Cambro-Ordovician quartz-phyllites, while originally the conglomerate should lie on top of the bedrock (Figs 5b-1 and 5b-2). In the central part of the landslide, large detached blocks are distributed all over the slope and show important rotations with opposite dips of stratum bedding. Figure 5b-3 thereby shows a conglomerate block with normal dip towards the West but which still is slightly rotated as the dip angle of up to 30° is clearly larger than the normal 10° dip angle of undisturbed conglomerate beds. Figure 5b-4 illustrates the stratum bedding of a completely overturned block, with stratum dip of $\sim 50\text{--}60^\circ$ towards the E. A pronounced geomorphic graben structure has been found in the upper part of the slope, indicating a clearly brittle behaviour the detached rock masses (Fig. 5b-5). This morphological setting of the site suggests a rather severe triggering event due to the relatively small average slope angle ($\sim 15^\circ$) and the originally gently dipping strata (about 10° towards the W, Fig. 5b-6).

Furthermore, the GIS results of Hillshade, Curvature and Slope analysis presented in Figure 6 were used to highlight characteristic features of the investigated surface. The prominent scarp with a strike of $N330^\circ E$ is clearly marked on the Hillshade raster in the north-western part of the landslide (Fig. 6a).

The hummocky morphology of the slope is particularly well represented by the alternation of concave and convex attributes in the Profile Curvature map (Fig. 6b). The Slope analysis (Fig. 6c) highlights important slope angles ($>50^\circ$) at the scarp, at the top (near the graben aperture in the NW of the landslide area) and on the opposite slope in the SE of the landslide area (most likely caused by small rivulets flowing around the landslide and eroding the opposite slope).

The Bévécé scarp, in particular, is characterised by a pronounced morphology; compared to other slopes in the region it is clearly steeper (slope $>50^\circ$), while other slopes within the conglomerate formation are less than 30° steep) and totally straight over a length of about 100 m. The orientation of the scarp is $N330^\circ E$ and aligns with the direction of the Trô Maret valley as well as with the general orientation of the eastern border faults of the HFZ.

For the geophysical prospection, results are presented in form of 2D tomographies (SRT and ERT). Figure 7 thereby shows the survey results of the scarp prospection, while Figure 8 presents a geoelectric profile that crosses the landslide body.

Figure 7 shows the results of SP05 vs. ERT03 and SP06 vs. ERT04 across the assumed fault scarp; the sections are marked by significant contrasts, both in terms of P-wave velocity and of electrical resistivity. For the P-wave profiles SP05 and SP06,

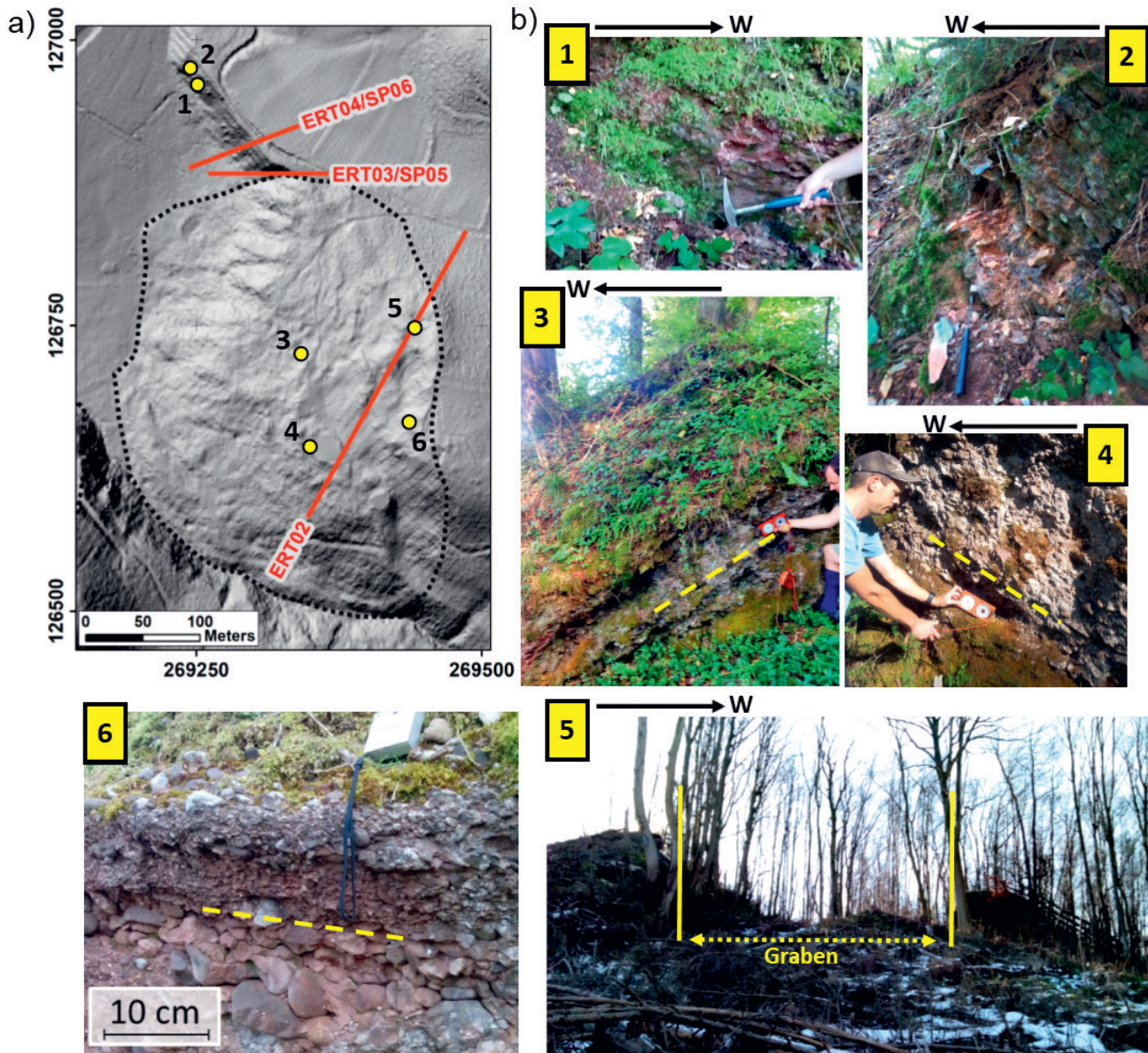


Figure 5. Structural analysis of the scarp and landslide area. a) Hillshade raster with location of outcrops shown in (b) as well as location of geophysical profiles (ERT04/SP06 and ERT03/SP05 along the scarp and ERT02 crossing the landslide, see results in Figs 7 and 8). b) Photographs of outcrops and the graben: 1 – Outcrop of the Malmedy Formation at the scarp; 2 – Outcrop of the quartz-phyllite bedrock at the scarp (in direct vicinity to ‘1’); 3 – Block with conglomerate strata dipping towards the W (i.e. original dip direction); 4 – Overturned block with strata dipping towards E (i.e. opposite to normal dip direction); 5 – Graben aperture at the top of the slope (head scarp and counter slope); 6 – Outcrop of the Malmedy Formation in its original layering (i.e. $10\text{--}15^\circ$ towards W).

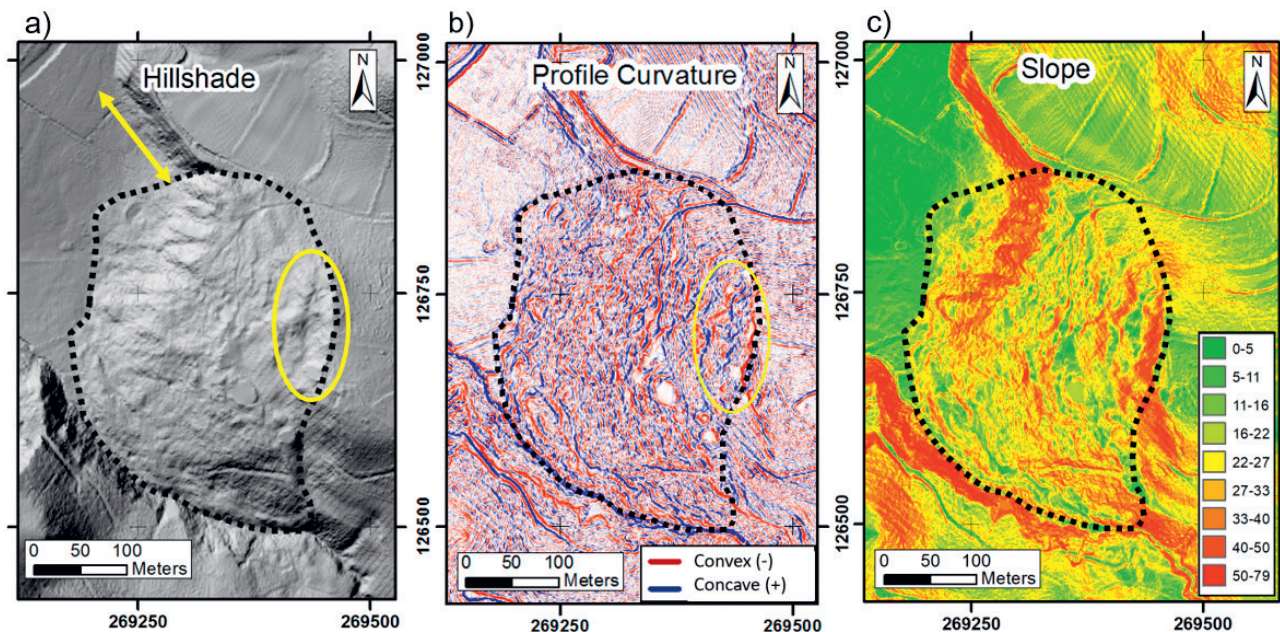


Figure 6. Analysis of the LiDAR-DEM (coordinate system: Belgian Lambert 72 projection): a) Hillshade raster presenting the fault scarp (along arrow) and geomorphic graben (circled) in the East part of the landslide. b) Profile Curvature highlighting the hummocky structure of the slope with alternating positive (upwardly concave) and negative (upwardly convex) profile curvatures (Profile Curvature definition after ESRI, 2015). c) Slope raster with green-red colour scheme indicating slope angles in degrees.

a lateral heterogeneity in the middle of the profile marking a vertical offset of the high velocity layers can be noticed (see Figs 7a and 7c). The electrical resistivity profiles ERT03 and ERT04 (Figs 7b and 7d) show a subvertical low resistivity zone ($<200 \Omega.m$) in the same place, between two areas marked by higher resistivities ($>300 \Omega.m$). The central part on these profiles highlighted by laterally changing P-wave velocities and lower electrical resistivities is interpreted as a zone of more intense rock fracturing subject to increased groundwater flow, probably due to the presence of a fault. By assigning the higher (>3500 m/s) P-wave velocities to the bedrock, we estimate that across this fault the bedrock was downthrown on the western side by about 15 m. The fault can therefore be considered as a normal fault (note that possible displacements along the strike of the fault plane could not be measured – such displacements would then indicate additional, possibly left-lateral, strike-slip movements). Moreover, the electrical survey ERT02 across the landslide body (Fig. 8) shows zones of lower resistivities surrounded by more resistive areas. These low resistivity zones marking the presence

of wet fractured rocks are located in the prolongation (along NNW-SSE strike) of the assumed fault scarp and thus indicate continuation of the fault across the mass movement, almost exactly where the main landslide scarp has developed.

5. Discussion

Although the here presented morphologies were only discovered recently, they can be considered as rather ancient features. The steep Bévécé scarp, in particular, is probably the product of the long-term tectonic activity of the region. With a strike of $N330^\circ E$ and located in the prolongation of the Trô Maret valley, this scarp is almost perpendicular to the predominant Variscan structures and those of the Malmedy Graben that have $N50-60^\circ E$ orientation. The same $N330^\circ E$ orientation can be observed for the abnormal course of the Paleo-Warthe crossing hard Cambrian rocks. The latter observation has been related by Demoulin et al. (2004) to the possible influence of the Hockai Fault Zone (HFZ). Through the geophysical prospecting of the Bévécé scarp we

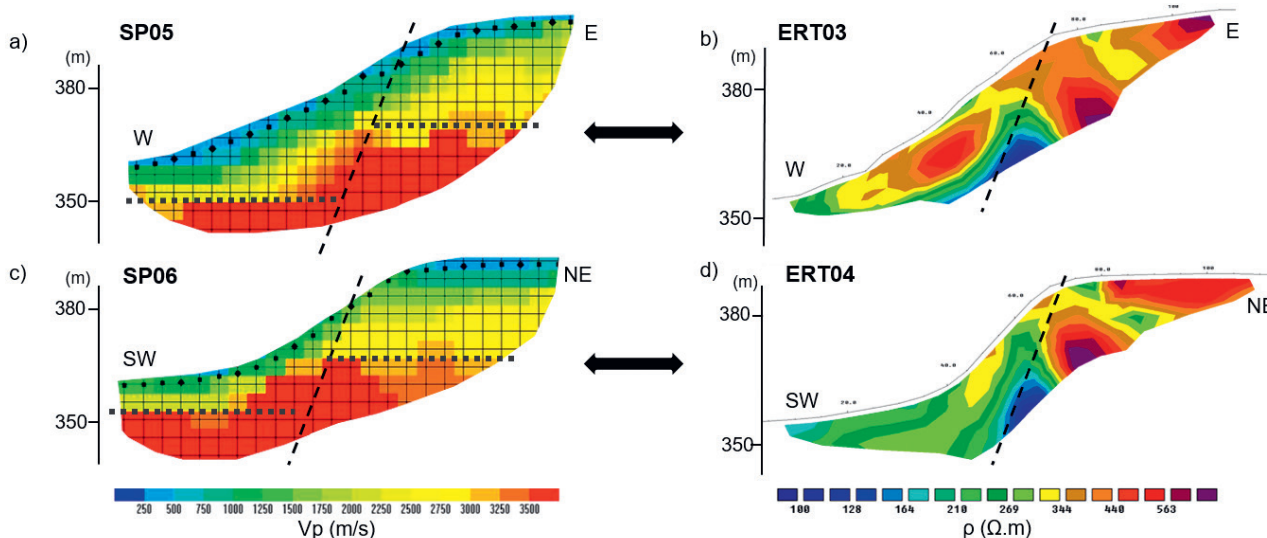


Figure 7. Comparison of seismic refraction and electrical resistivity measurements at two locations along the assumed fault scarp adjacent to the Bévécé landslide: SP05 (a) vs. ERT03 (b) and SP06 (c) vs. ERT04 (d). See survey locations in Figure 5a; dashed lines outline the location of the supposed fault plane.

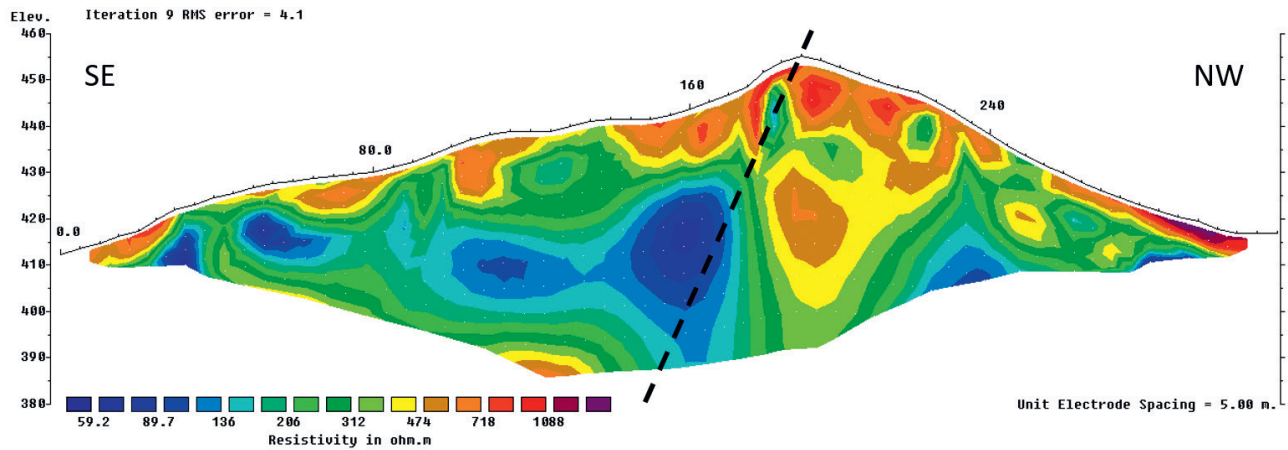


Figure 8. ERT02 crossing the landslide body from SE to NW along 315 m. A zone of weak electrical resistivities ($<150 \Omega.m$) corresponding to the location of prolonged scarp is marked by the dashed line (see survey location in Fig. 5a).

could clearly identify a ~ 15 m vertical displacement of the block marked by elevated P-wave velocities (>3500 m/s, assigned to the bedrock) as well as a zone of reduced electrical resistivity at the same location. This vertical shift zone is marked by low electrical resistivities indicating the presence of wet fractured rocks. These observations hint at the existence of a major normal fault along which the western block was downthrown. Related tectonic movements have probably occurred over many thousand years, but the landslides in the immediate vicinity of the scarp are likely to be much younger, probably less than 1000 years, but more than 100 years (as inferred from the various markers highlighted above). These landslides and the graben on top of the larger landslide could have been induced by relatively recent seismic events along that fault. Especially, the graben delimited by almost vertical well-cut rock scarps indicates an instantaneous trigger event producing brittle failure. Local recent movements (activations) in the north-western part of the large landslide are, however, due to climatic effects. Actually, an alluvial plain is located between the landslides and the river, though landsliding due to river erosion at the foot of the slope can be excluded. Also, karstic phenomena (such as those described elsewhere in the region by Ozer, 1979) can be excluded as possible trigger processes for the landslides, as those would not explain the numerous tilted and overturned conglomerate blocks (with altered dip of stratum bedding) and the clear opposite scarps of the geomorphic graben on top of the larger landslide. However, it is possible that local karstic erosion facilitated slope failure development. Considering the relatively gentle average slope of about 17° for the larger landslide area, a very strong seismic event would have been necessary to trigger such massive slope failures in intact conglomeratic rocks; such strong events might also have been accompanied by the most recent surface rupturing along the scarp, keeping its morphology relatively fresh. Such strong seismic shocks (probably much larger than the 1692 earthquake, with a magnitude of more than 6.5) are unlikely or, at least, very rare for the region. If we assume a more likely M6-6.5 earthquake as trigger of the two landslides (or several events?), we must also assume some long term weakening of subsurface strata before final failure, possibly induced by dissolution processes. Additional studies are needed to confirm these assumptions.

If the Malmedy features are compared with other slope failures along the HFZ, notably the *Pays de Herve* landslides in the Battice region, it can be noticed that they developed in a completely different environment. First, the geological setting of the landslides near Battice is more favourable to landsliding due to the presence of the clayey soft layers of the Vaals Formation (Upper Campanian) that are sensitive to water pressure changes and, especially within the landslide zones, are locally underlain by the Aachen Sands with a high liquefaction potential, as shown by Demoulin et al. (2003; see also Dewitte et al., 2018). Second, the *Pays de Herve* landslides developed in a rather smooth landscape, with slope angles rarely exceeding 12° . But even more striking is the number of 15 landslides in the rather restricted area

(~ 15 km 2); to explain this, Demoulin et al. (2003) suggested that they probably initiated simultaneously (i.e. 50–250 AD) due to the combination of climatic and seismic factors. For our study area, a larger number of slope failures would be expected in the case of a dynamic trigger as the slopes are generally much steeper than in the Battice region; however, only those two cases previously presented could have been identified in the Malmedy Graben so far. Reasons for this could be that no other slope in the vicinity provides similar conditions: the geographical position, as the presented landslides directly “sit” on the fault, but also the lithological setting, i.e. thick Permian layers on top of the faulted bedrock that provide enough material to create such massive and deep-seated landslides. Similar to the *Pays de Herve*, the combination of climatic and seismic events should be considered. However, as mentioned before, initiation by purely climatic factors is considered as rather unlikely for the Bévercé landslides (due to the presence of numerous brittle deformation features).

Even though seismic events associated with recent fault movements best explain the formation of the landslides, we do not claim that the present-day height and ‘fresh-looking’ morphology of the scarp is purely connected with modern seismotectonics ($<10,000$ years). Considering the geomorphic context of the area, it is very likely that a ‘weak’ zone had formed over a much longer period along the eastern border of the HFZ. Most of it was buried below the conglomeratic filling of the Malmedy Graben, probably with little surface expression. Due to the capture of the Warche River and the related accelerated erosion of the graben filling (also by neighbouring rivers, such as the Trô Maret) that has started about 50,000–80,000 years ago, the buried weak zone was denudated and successively became a scarp. The present-day strong morphology of the scarp is therefore most likely due to the relatively young age of the denudation of the weakened zone near the eastern border of the HFZ – and (mostly) not to an accumulation of vertical surface displacements due to very recent tectonic movements (as known from other far more active fault zones). Though, as mentioned above, relatively recent surface rupturing (<1000 years BP, with displacements of about 1 m) would help explain the fresh looking morphology of the scarp, which is exceptional for a region marked by a low to medium seismotectonic activity.

6. Conclusions

The geomorphological study of the Bévercé scarp and slope failure structures provided new information on the recent seismotectonic history of the Malmedy region. The steep, 20 m high and 100 m long, scarp as well as the adjacent Trô Maret valley in the North are both located along the eastern border of the seismically active Hockai Fault Zone. Field observations on the larger of the two landslides show important morphological and structural markers that indicate a massive and relatively rapid slope failure. The geophysical profiles along the scarp show vertical normal displacements of the bedrock across the scarp that may therefore be considered as a fault scarp. The presence of

this fault scarp and of slope movements indicating rapid trigger processes suggests a seismic origin of at least the larger landslide (the second one still needs to be studied more in detail). It is most likely that a seismic activation of the HFZ was responsible for this trigger. In order to confirm this assumption, further geophysical investigations on the landslides as well as numerical modelling of dynamic slope failure processes would be needed. Further, it is intended to launch a survey aiming at dating of samples from the scarps and the landslide bodies as the age of the observed geomorphic and tectonic features are still unknown. It is only expected that the scarp developed over thousands of years (and the originally buried weak zone over tens of thousands of years) while the landslides have probably been triggered several hundreds of years ago.

7. Acknowledgement

We would like to thank the Fund for Research Training in Industry and Agriculture (FRIA/F.R.S.-FNRS, Belgium) for supporting Anne-Sophie Mreyen with a PhD fellowship. We thank the group of Prof. Frédéric Nguyen, Liege University, Belgium, for the ABEM system we used to complete the long ERT02 profile. Furthermore, we thank Jean-Marc Marion for the indication of the presence of the Bévercé landslide and the access to his geological map before publication of the same – it was re-digitized by the first author. Last but not least, we kindly thank the reviewers, Olivier Dewitte (Royal Museum for Central Africa, Tervuren, Belgium) and Martin Salamon (Geological Survey of North Rhine-Westphalia, Germany), who helped to improve the quality of this paper.

8. References

- Ahorer, L., 1983. Historical seismicity and present-day microearthquake activity of the Rhenish Massif, Central Europe. In Fuchs, K., von Gehlen, K., Mälzer, H., Murawski, H. & Semmel, A. (eds), *Plateau Uplift: The Rhenish Shield – A Case History*. Springer, Berlin, 198–221.
- Alexandre, P., Kusman, D., Petermans, T. & Camelbeeck, T., 2008. The 18 September 1692 earthquake in the Belgian Ardenne and its aftershocks. In Fréchet, J., Meghraoui, M. & Stucchi, M. (eds), *Historical Seismology: Interdisciplinary Studies of Past and Recent Earthquakes*. Springer, Dordrecht, 209–230. https://doi.org/10.1007/978-1-4020-8222-1_10
- Ancion, C. & Evrard, E., 1957. Contribution à l'étude des failles Monty, Mouhy et d'Ostend dans la partie orientale du Massif de Herve. *Annales de la Société Géologique de Belgique*, 80, B477–B488.
- Antun, P., 1954. La période continentale posthercynienne : le poudingue de Malmédy et formations analogues. In Fourmarier, P. (ed.), *Prodrome d'une description géologique de la Belgique*. Société Géologique de Belgique, Liège, 369–375.
- Barchy, L. & Marion, J.-M., 2000. Carte géologique de Wallonie : Dalhem – Herve 42/3-4. 1/25 000. Namur, Ministère de la Région wallonne, Direction générale des ressources naturelles et de l'environnement, avec une notice explicative de 71 p.
- Bless, M.J.M., Bouckaert, J., Camelbeeck, T., Dejonghe, L., Demoulin, A., Dupuis, C., Felder, P.J., Geukens, F., Gullentops, F., Hance, L., Jagt, J.W.M., Juvigné, E., Kramm, U., Ozer, A., Pissart, A., Robaszynski, F., Schumacker, R., Smolderen, A., Spaeth, G., Steemans, Ph., Streel, M., Vandeven, G., Vanguetaine, M., Walter, R. & Wolf, M., 1990. The Stavelot massif from Cambrian to recent. A survey of the present state of knowledge. *Annales de la Société Géologique de Belgique*, 113/2, 53–73.
- Camelbeeck, T., 1993. Mécanisme au foyer des tremblements de terre et contraintes tectoniques: le cas de la zone intraplaque belge. Unpublished PhD thesis. Université Catholique de Louvain, Belgium, 295 p.
- Camelbeeck, T., Alexandre, P., Vanneste, K. & Meghraoui, M., 2000. Long-term seismicity in regions of present day low seismic activity: the example of western Europe. *Soil Dynamics and Earthquake Engineering*, 20/5, 405–414. [http://dx.doi.org/10.1016/S0267-7261\(00\)00080-4](http://dx.doi.org/10.1016/S0267-7261(00)00080-4)
- Challis, K., Forlin, P. & Kincey, M., 2011. A generic toolkit for the visualization of archaeological features on airborne LiDAR elevation data. *Archaeological Prospection*, 18/4, 279–289. <http://dx.doi.org/10.1002/arp.421>
- Cunningham, D., Grebby, S., Tansey, K., Gosar, A. & Kastelic, V., 2006. Application of airborne LiDAR to mapping seismogenic faults in forested mountainous terrain, southeastern Alps, Slovenia. *Geophysical Research Letters*, 33/20, L20308. <http://dx.doi.org/10.1029/2006GL027014>
- Delvenne, Y., Demoulin, A. & Juvigné, E., 2004. L'évolution géomorphologique dans le secteur de l'ancienne confluence Warche-Trô Maret. *Hautes Fagnes*, 2004/4, 256, 101–105.
- Demonet, D., 2000. Tomographies 2D et 3D à partir de mesures géophysiques en surface et en forage. Unpublished PhD thesis. Université de Liège, Belgium, 153 p.
- Demoulin, A., 1988. Cenozoic tectonics on the Hautes Fagnes plateau (Belgium). *Tectonophysics*, 145/1-2, 31–41. [https://doi.org/10.1016/0040-1951\(88\)90313-7](https://doi.org/10.1016/0040-1951(88)90313-7)
- Demoulin, A., 2006. La néotectonique de l'Ardenne-Eifel et des régions avoisinantes. *Académie Royale de Belgique, Mémoires de la Classe des Sciences*, in 8°, 25, 252 p.
- Demoulin, A. & Chung, C.-J.F., 2007. Mapping landslide susceptibility from small datasets: A case study in the Pays de Herve (E Belgium). *Geomorphology*, 89/3-4, 391–404. <http://dx.doi.org/10.1016/j.geomorph.2007.01.008>
- Demoulin, A. & Glade, T., 2004. Recent landslide activity in Manaihan, East Belgium. *Landslides*, 1/4, 305–310. <http://dx.doi.org/10.1007/s10346-004-0035-z>
- Demoulin, A., Pissart, A., Poty, E., Barchy, L., Marion, J.M. & Chung C.F., 2000. Les glissements de terrain du Pays de Herve. Unpublished report. Ministère de la Région wallonne, Namur, 146 p.
- Demoulin, A., Pissart, A. & Schroeder, C., 2003. On the origin of late Quaternary palaeolandslides in the Liège (E Belgium) area. *International Journal of Earth Sciences*, 92/5, 795–805. <http://dx.doi.org/10.1007/s00531-003-0354-7>
- Demoulin, A., Delvenne, Y. & Juvigné, E., 2004. Les cours hypothétiques de la Warche pendant le Tertiaire et le Quaternaire ancien. *Hautes Fagnes* 2004/3, 255, 80–83.
- Dewitte, O., Van Den Eeckhaut, M., Poesen, J. & Demoulin, A., 2018. Landslides in Belgium—Two case studies in the Flemish Ardennes and the Pays de Herve. In Demoulin, A. (ed.), *Landscapes and Landforms of Belgium and Luxembourg*. Springer, Cham, 335–355. https://doi.org/10.1007/978-3-319-58239-9_20
- Dumont, A.H., 1832. Mémoire sur la constitution géologique de la province de Liège. *Mémoires couronnés et mémoires des savants étrangers de l'Académie des Sciences et Belles-Lettres de Bruxelles*, 8, 374 p.
- ESRI, 2015. ArcGIS 10.3 Desktop Help. ESRI, Redlands, CA.
- Forir, H., 1905. Le pays de Herve. Essai de géographie physique. *Annales de la Société Géologique de Belgique*, 33, M163–M171.
- Geukens, F., 1957. Les failles bordières du Graben de Malmédy. *Bulletin de la Société Belge de Géologie*, 66, 71–81.
- Geukens, F., 1995. "Strike slip deformation" des deux côtés du Graben de Malmédy. *Annales de la Société Géologique de Belgique*, 118/2, 139–146.
- Juvigné, E. & Delvenne, Y., 2005. La capture de la Warche entre Bévercé et Mont-Xhoffraix. *Hautes Fagnes*, 2005/1, 257, 21–25.
- Juvigné, E. & Schumacker, R., 1985. Données nouvelles sur l'âge de la capture de la Warche à Bévercé. *Bulletin de la Société géographique de Liège*, 21, 3–11.
- Lamberty, P., Geukens, F. & Marion, J.-M., in press. Carte géologique de Wallonie : Stavelot – Malmédy 50/5-6. 1/25 000. Namur, Service Public de Wallonie, avec une notice explicative.
- Lecocq, T., 2011. L'activité sismique en Ardenne et sa relation avec la tectonique active. Unpublished PhD thesis. Université libre de Bruxelles, Belgium, 265 p.
- Lin, Z., Kaneda, H., Mukoyama, S., Asada, N. & Chiba, T., 2013. Detection of subtle tectonic–geomorphic features in densely forested mountains by very high-resolution airborne LiDAR survey. *Geomorphology*, 182, 104–115. <http://dx.doi.org/10.1016/j.geomorph.2012.11.001>
- Loke, M.H., 2004. Tutorial: 2-D and 3-D electrical imaging surveys. *Geotomo Software*, Malaysia, 128 p.
- Loke, M.H. & Barker, R.D., 1996. Practical techniques for 3D resistivity surveys and data inversion. *Geophysical prospecting*, 44/3, 499–523. <https://doi.org/10.1111/j.1365-2478.1996.tb00162.x>
- Ozer, A., 1967. Contribution à l'étude géomorphologique des régions où affleure "le Poudingue de Malmédy." Unpublished Master thesis. Université de Liège, Belgium, 180 p.
- Ozer A., 1979. Les phénomènes karstiques développés dans le Poudingue de Malmédy. *Annales de Spéléologie*, 26, 407–422.
- Ozer A. & Macar P., 1968. Le poudingue de Malmédy occupe-t-il un graben ? *Annales de la Société Géologique de Belgique*, 91, 559–568.
- Pissart, A. & Juvigné, E., 1982. Un phénomène de capture près de Malmédy : la Warche s'écoulait autrefois par la vallée de l'Eau Rouge. *Annales de la Société Géologique de Belgique*, 105, 73–86.
- Prick A. & Ozer A., 1995. Les paysages physiques de l'Ardenne. In Demoulin A. (Ed.), *L'Ardenne : essai de géographie physique*. Département de Géographie physique et Quaternaire, Université de Liège, Liège, 31–52.
- Renier, A., 1902. Le poudingue de Malmédy – Essai géologique. *Annales*

- de la Société Géologique de Belgique, 29, M145–M223.
- Rixhon, G. & Demoulin, A., 2018. The picturesque Ardennian valleys: Plio-Quaternary incision of the drainage system in the uplifting Ardenne. In Demoulin, A. (ed.), *Landscapes and Landforms of Belgium and Luxembourg*. Springer, Cham, 159–175. https://doi.org/10.1007/978-3-319-58239-9_10
- Service Public de Wallonie (SPW), 2015. IMAGERIE/ORTHO_2015 (MapServer). Retrieved 2016-03-01 from http://geoservices.wallonie.be/arcgis/rest/services/IMAGERIE/ORTHO_2015/MapServer.
- Vanneste, K., Camelbeeck, T., Verbeeck, K. & Demoulin, A., 2018. Morphotectonics and past large earthquakes in Eastern Belgium. In Demoulin, A. (ed.), *Landscapes and Landforms of Belgium and Luxembourg*. Springer, Cham, 215–236. https://doi.org/10.1007/978-3-319-58239-9_13